Talanta 208 (2020) 120338

Contents lists available at ScienceDirect

Talanta

journal homepage: www.elsevier.com/locate/talanta

Nanostructured impedimetric lectin-based biosensor for arboviruses detection

Estefani P. Simão[a], Dammyres B.S. Silva[b], Marli T. Cordeiro[c], Laura H.V. Gil[c], Cesar A.S. Andrade[b], Maria D.L. Oliveira[a,b,*]

[a] Programa de Pós-Graduação em Ciências Biológicas, Universidade Federal de Pernambuco, 50670-901, Recife, PE, Brazil
[b] Departamento de Bioquímica, Universidade Federal de Pernambuco, 50670-901 Recife, PE, Brazil
[c] Departamento de Virologia-Instituto Aggeu Magalhães-Fiocruz, 50670-420, Recife, PE, Brazil

ARTICLE INFO

Keywords:
Concanavalin A
Nanoparticles
Arboviruses
Biosensor
Impedance spectroscopy

ABSTRACT

Arboviruses have been emerging as a significant global health problem due to the recurrent epidemics. Arboviruses require the development of new diagnostic devices due to the nonspecific clinical manifestations. Herein, we report a biosensor based on cysteine (Cys), zinc oxide nanoparticles (ZnONp), and Concanavalin A (ConA) lectin to differentiate between arboviruses infections. ConA is capable of interacting with the saccharide components of the viral capsid. In this study, we evaluated the reproducibility, sensitivity, and specificity of the sensor for the virus of Dengue type 2 (DENV2), Zika (ZIKV), Chikungunya (CHIKV), and Yellow fever (YFV). Atomic force microscopy measurements confirmed the electrode surface modification and revealed a heterogeneous topography during the biorecognition process. Cyclic voltammetry (CV) and impedance spectroscopy (EIS) were used to characterize the biosensor. The blockage of the oxidation-reduction process is related to the formation of Cys-ZnONp-ConA system on the electroactive area and its subsequent interaction with viral glycoproteins. The sensor exhibited a linear response to different concentrations of the studied arboviruses. Our study demonstrates that ConA lectin recognizes the structural glycoproteins of the DENV2, ZIKV, CHIKV, and YFV. DENV2 is the most structurally similar to ZIKV. Our results have shown that the impedimetric response correlates with the structural glycoproteins, as follow: DENV2 (18.6 kΩ) > ZIKV (14.6 kΩ) > CHIKV (6.86 kΩ) > YFV (5.98 kΩ). The homologous structural regions contribute to ConA-arboviruses recognition. Our results demonstrate the use of the proposed system for the development of biosensors for arboviruses infections.

1. Introduction

Dengue (DENV), Zika (ZIKV), Chikungunya (CHIKV), and Yellow Fever (YFV) viruses are arboviruses (arthropod-borne viruses) associated to worldwide outbreaks and a significant public health problem [1–3]. DENV, ZIKV, and YFV are single-stranded RNA viruses of the *Flaviviridae* family and genus *Flavivirus*. These arboviruses contain an internal matrix protein and a surface glycoprotein to mediate interactions. Also, the virus has structural (E, C, and M) and non-structural (NS) proteins. CHIKV is an RNA virus belonging to the genus *Alphavirus* of the *Togaviridae* family. CHIKV structural proteins are different from the other arboviruses due to the presence of two surface glycoproteins (E1 and E2) [4,5]. DENV2 is the most structurally similar to ZIKV due to the presence of homologous structural regions [6]. ZIKV presents radial distances of the lipid bilayer core, and its envelope ectodomains are similar to those of DENV2 [7].

The arboviruses are structurally composed of glycoproteins and glycolipids, both with extreme importance for the infection process and penetration of the virus into the host cell [8]. The glycans are significant components of the outermost surface of the virus. The structural glycoproteins of the DENV, ZIKV, CHIKV, and YFV are composed of mannose, galactose, and N-acetylglucosamine [7,9,10].

DENV, ZIKV, CHIKV, and YFV are challenging to be diagnosed clinically due to similarities in the symptoms [11]. The late immune stimulus and similarity between the arboviruses are associated with cross-reactions in immunological tests (e.g., MAC-ELISA) [13]. Reverse transcription-quantitative real-time polymerase chain reaction (RT-qPCR) is also used to identify arboviruses. RT-qPCR is useful to detect the virus RNA at the early stage of the infection; after this period, the number of false negatives increases [14].

* Corresponding author. Departamento de Bioquímica, UFPE, 50670-901, Recife, PE, Brazil.
E-mail address: m_danielly@yahoo.com.br (M.D.L. Oliveira).

https://doi.org/10.1016/j.talanta.2019.120338
Received 3 June 2019; Received in revised form 4 September 2019; Accepted 5 September 2019
Available online 06 September 2019
0039-9140/

On the other hand, previous studies have demonstrated the applicability of biosensors as diagnostic methods for arboviruses [15–17]. Electrochemical impedance spectroscopy (EIS) and cyclic voltammetry (CV) techniques associated with nanostructures have been extensively used for the development of biosensors [18,19]. Graphene, carbon nanotubes, carbon dots, and metallic nanoparticles are nanomaterials with outstanding characteristics such as electron transfer, chemical stability, and thermal conductivity [20–24]. Nanomaterials are widely used in electrochemical biosensors due to their high surface area, electrochemical activity, and the possibility of functionalization [25,26]. Zinc oxide nanoparticles (ZnONp) can optimize the electrochemical responses due to fast electron transfer capability and biocompatibility [19,27].

Lectins are attractive biorecognition molecules for the development of biosensors due to their specific interaction properties with free or conjugated carbohydrate residues. Lectins have demonstrated the potential for use in virus detection in human serological samples [28–30]. Concanavalin A (ConA) is a carbohydrate-binding protein with monosaccharide specificity (Gly/Man). ConA is capable of differentiating glycoproteins presents in serum from arbovirus-infected patients and normal serum [31]. Lectins have shown potential for the development of new nanostructured platforms for arboviruses detection [17,32,33].

Herein, we report a new sensitive electrochemical biosensor based on a self-assembled monolayer of ConA lectin and ZnONp for detection of mannose-glucose residues present in DENV2, ZIKV, CHIKV, and YFV. Fig. 1 shows the proposed sensor platform for the diagnosis of arboviral infections.

2. Methodology

2.1. Materials

ConA lectin, bovine serum albumin (BSA), ZnONp, cysteine (Cys), 1-[3-(dimethylamino)propyl]-3-ethylcarbodiimide hydrochloride (EDC), N-hydroxysuccinimide (NHS), and aminopropyltriethoxysilane (APTES) were purchased from Sigma Chemical (St. Louis, MO, USA). Potassium ferri- and ferrocyanide were obtained from VETEC (Brazil). All chemicals were of analytical grade and used as received without further purification. Ultrapure water was obtained from a Millipore Milli-Q system. Arbovirus strains and serum (from healthy and arbovirus-infected patients) were provided from the Department of Virology of the Institute Aggeu Magalhães.

2.2. Electrode modification

ZnONp were functionalized with APTES according to the method described by Grasset et al. [34]. The bare gold electrode was polished with alumina, rinsed with deionized water, and dried at room temperature. Subsequently, 2 µL of Cys (70 mM) was used to obtain a self-assembled monolayer on the electrode surface. Then, 2 µL of a solution containing 0.4 M EDC and 0.1 M NHS (1:1, v/v) was added to the electrode surface for 10 min. Subsequently, 2 µL of ZnONp was dropped on the Cys-EDC/NHS-modified electrode surface. After, the sensor layer was prepared by dropping 2 µL of ConA (1 mg mL^{-1}) on the electrode surface and incubated for 10 min. Finally, 2 µL of BSA (10%) was used in all experiments to avoid non-specific interactions. The performance of the biosensor was assessed using 2 µL of ZIKV, CHIKV, DENV2, or YFV in a dilution 1:10 with an incubation time of 10 min.

2.3. Dengue, Zika, Chikungunya, and yellow fever viruses

The Department of Virology of the Institute Aggeu Magalhães (IAM – FIOCRUZ) provided the viruses used in this study. DENV2, ZIKV, and CHIKV were isolated from newly infected patients of the state of Pernambuco, molecularly identified and characterized, as follows: DENV2 - BRPE/95-3808; ZIKV - BRPE243/2015; and, CHIKV - BRPE480/2016. The yellow fever virus was the attenuated YF-17DD vaccine strain. In this study, we used a strain of attenuated yellow fever virus (YF-17DD vaccine). Patients with characteristic clinical symptoms donated blood samples. The specimens were spun down for 10 min at $1500 \times g$ and stored at −80 °C. Serum samples were submitted to molecular diagnostic assays for the detection of ZIKV, DENV, and chikungunya virus (CHIKV). The viruses strains were propagated in Vero cells (African green monkey kidney), titrated, and kept stored at −80 °C. The viruses were inactivated with BPL (Beta propiolactone) before use. Plaque reduction neutralization test (PRNT) was used to detect ZIKV at different concentrations (Fig. S1). PRNT50 is defined as the reciprocal of the highest test serum dilution at which the virus infectivity is reduced by 50% [35].

2.4. Electrochemical measurements

Electrochemical measurements were performed using a conventional three-electrode system interfaced with a PGSTAT 128N potentiostat/galvanostat (Metrohm Autolab Inc., Netherlands). The electrical circuit analysis was performed with the NOVA 1.11 software. The

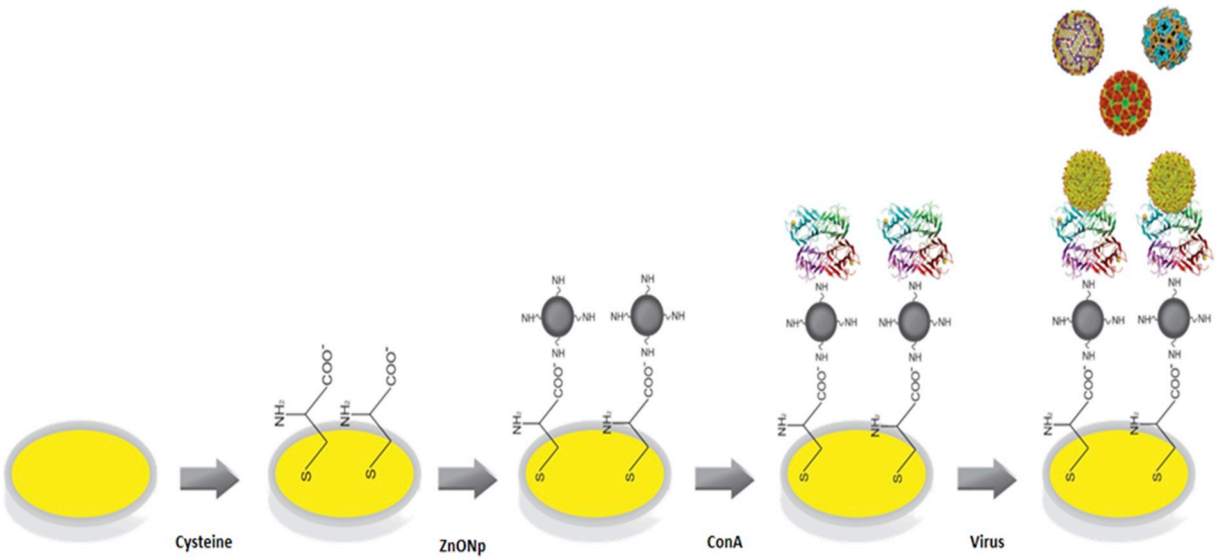

Fig. 1. Schematic representation of the surface modification.

working electrode was a bare gold electrode and a platinum wire and Ag/AgCl electrode saturated with KCl (3 M) were used as counter and reference electrodes, respectively. The impedance spectra were recorded in the 100 mHz and 100 kHz frequency range with an alternating voltage adjusted to an amplitude of 10 mV. The CV analysis was performed in the −0.2 V and +0.7 V potential range at a scan rate of 50 mV s^{-1}. The electrolytic solution was 10 mM $K_4[Fe(CN)_6]^{4-}/K_3[Fe(CN)_6]^{3-}$ (1:1, v/v) in 10 mM PBS (pH 7.4). All electrochemical measurements were performed in triplicate (n = 3) using three independent electrodes to evaluate the reproducibility. The electrochemical experiments were performed at room temperature inside a Faraday cage.

2.5. Atomic force microscopy measurements

Topographic analyses were performed with an SPM9700 atomic force microscope (Shimadzu Instruments Co. Ltd, Japan) in a non-contact mode at room temperature (~25 °C). Cantilevers with a silicon AFM probes (Nanoworld, Japan, resonant frequency = 190 kHz, spring constant = 42 N m^{-1}) were used. The images (512 points per line) were collected with a scan rate of 1.0 Hz in a scan area of 5 × 5 μm. Gwyddion software was used for analysis and processing of the images [36].

3. Results and discussion

3.1. Topographic characterization

AFM technique was used to evaluate the morphology of the Cys-ZnONp-ConA film and arboviruses recognition. Fig. 2 shows AFM topographic images of the sensor surface.

A different covering of the electrode surface was obtained for Cys-ZnONp (Fig. 2a) and Cys-ZnONp-ConA (Fig. 2b) systems with a mean height of 37 ± 2.1 nm and 47 ± 1.5 nm, respectively. These results are following previous studies that determined the height of ~12 nm for the ConA tetramer [37]. The recognition of viral surface glycoproteins by ConA is shown in Fig. 2c–f. Cys-ZnONp-ConA system showed the weakest interaction to YFV (mean height of 63.0 ± 3.4 nm) as compared to the other studied arboviruses (Fig. 2c). A dense adsorbed layer on the sensor surface was obtained for DENV2, ZIKV, and CHIKV with mean heights of 75 ± 2.4 nm, 260 ± 3.9 nm, and 72 ± 1.2 nm, respectively (Fig. 2d–f). The difference observed in the height data is attributed to the specificity of ConA lectin to the viral glycoproteins [38,39].

3.2. Electrochemical characterization

Fig. 3a shows the cyclic voltammograms of the oxidation/reduction peaks of the redox pair and assembly process of the sensor. The bare gold electrode showed quasi-reversible redox behavior. A decrease in the amperometric current is obtained after addition of Cys molecules on the gold electrode surface. This behavior is due to the chemical interaction between Cys and gold surface through the thiol group (-SH) [40,41]. The peak currents increased with the aminated ZnONp concentration. The ZnONp adsorption occurs through EDC:NHS. The coupling agents activate negative charge terminal carboxyl group of Cys that is substituted by NHS ester on the electrode surface. Thus, the accumulation of positive charges on the electrode surface attracts the redox probe [18,19]. ConA is adsorbed on the Cys-ZnONp surface through electrostatic interaction. After, a decrease in the amperometric current is observed associated with the physical adsorption of the lectin [42,43]. BSA solution was employed to block remaining active sites on the electrode surface [40]. The redox peak currents decreased after addition of BSA.

Fig. 3b shows a typical Nyquist plot of the modification of the electrode surface. The impedance data were fitted with NOVA 1.8 software by using modified Randles equivalent model (inset of Fig. 3b). The circuit includes a solution resistance (Rs), charge transfer resistance (Rct), Warburg impedance element (Zw), and phase constant element (Q). The diameter of the semicircle represents the values of the Rct.

The bare gold electrode spectrum is characterized by a small semicircle at a high-frequency domain and a low R_{CT} value (Rct = 0.35 kΩ) [17]. An increase of the Rct (4.79 kΩ) was observed after addition of Cys molecules. Conversely, the immobilization of the ZnONp results in a decrease of the Rct (0.66 kΩ) due to a rapid electron transfer kinetics [18]. A further increase in the Rct (2.34 kΩ) was obtained after the addition of ConA due to an effective immobilization of the lectin to the developed nanostructured platform. The magnitude of the impedimetric response increases to 5.34 kΩ after the immobilization of BSA onto modified electrode. EIS results were in good agreement with those from CV measurements confirming the surface modification.

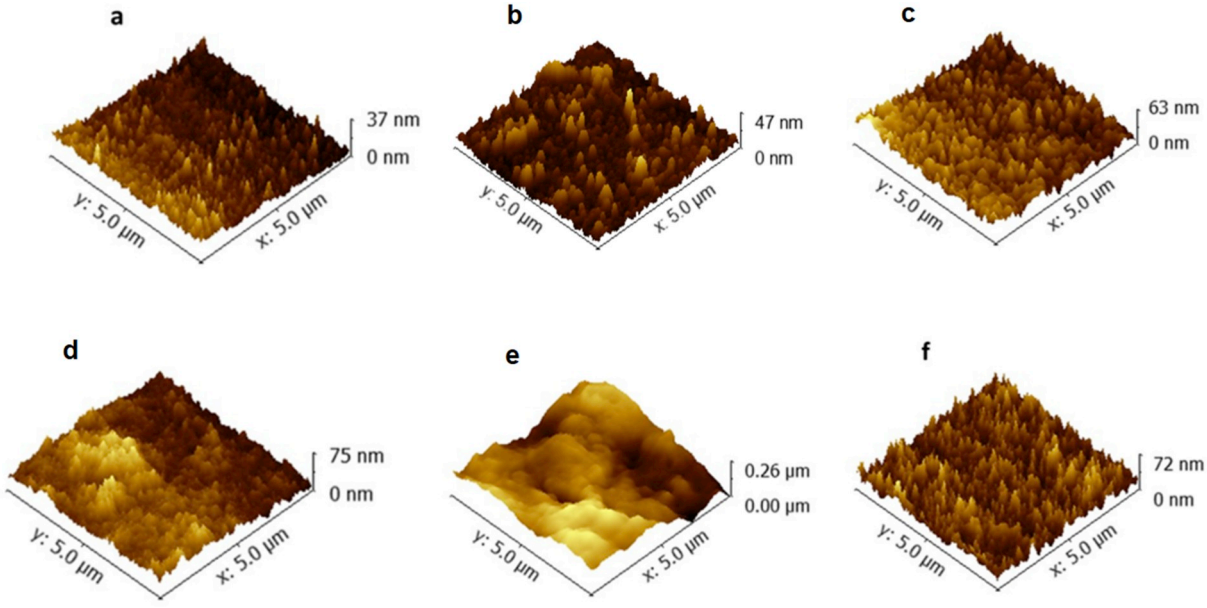

Fig. 2. AFM images of the stepwise modification process: (a) Cys-ZnONp-ConA-BSA, (b) Cys-ZnONp-ConA-BSA-DENV, (c) Cys-ZnONp-ConA-BSA-CHIKV, (d) Cys-ZnONp-ConA-BSA-ZIKV, and (e) Cys-ZnONp-ConA-BSA-YFV.

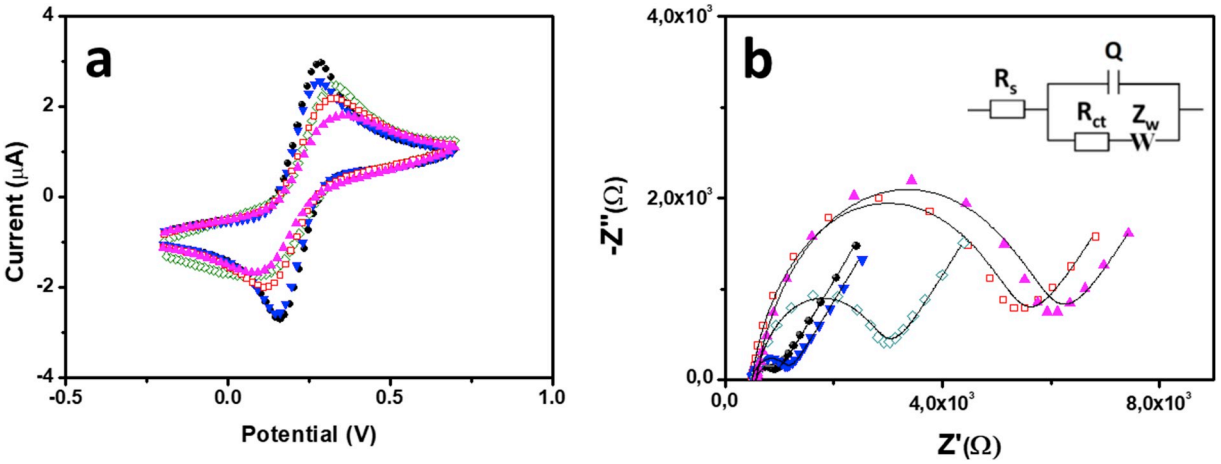

Fig. 3. Cyclic voltammogram (a) and Nyquist diagram (b) of the stepwise modification process: (•) gold electrode, (□) Cys, (▽) ZnONp, (⋄) ConA, and (Δ) BSA. (For interpretation of the references to colour in this figure legend, the reader is referred to the Web version of this article.)

The specificity of ConA was evaluated against lactose and glycogen as negative controls. Lactose is a disaccharide composed of glucose and galactose. Glycogen is a polysaccharide consisting of glucose residues. ConA has specificity for non-reducing α-D-mannosyl and α-D-glycosyl groups. The electrochemical measurements for lactose and glycogen recognition displayed no significant response (Fig. S2).

The biological activity of the Cys-ZnONp-ConA-BSA platform was evaluated against glycoproteins (fetuin and ovalbumin) (Fig. S3). The impedance values increase after the exposition of the sensor to these glycoconjugates. Thus, ConA was capable of recognizing fetuin and ovalbumin. Similar results have been previously obtained by other authors [32]. The lectin-glycoprotein complex can act as the inert electron and mass transfer-blocking layer. Therefore, this complex hinders the movement of ferricyanide toward the electrode surface.

3.3. Analytical performance of the biosensor on real samples

Differences in the viral envelope are an essential characteristic of the differentiation of the immunological response after infection by arboviruses. The structural components of the viral envelope can be used to identify and differentiate arboviruses [9]. Thus, ConA lectin was used in this work for the identification and differentiation of the carbohydrates on the viral envelope.

The electrochemical response of the sensor to DENV2, ZIKV, CHIKV, and YFV is shown in Fig. 4. The degree of affinity of the sensor to the virus decreased from ZIKV > DENV2 > CHIKV > YFV. The sensor shows the highest response to ZIKV due to the interaction of ConA with specific residues of carbohydrates present in structural glycoprotein E of the ZIKV [8,44]. The DENV2 showed increased interaction with ConA due to the presence of glycans on its surface. Carbohydrates residues distributed on ZIKV surface differ in density and conformation as compared to DENV2 [7].

The binding between ConA and viral glycoproteins reflects the interaction of the biomolecule with residues of carbohydrates present in the Ans^{154} glycan monomer exposed on the surface of the DENV2 and ZIKV viruses [7]. CHIKV is composed of a glycidic structure containing mannose sugars, which favors the lectin interaction and results in an increase of the resistivity [45].

ConA lectin recognizes ZIKV due to positive charges in the central and negative regions in the distal portion of the non-structural protein 1 (NS1) of the virus. The charge distribution of the DENV2 NS1 protein is different from ZIKV. Besides, DENV2 NS1 protein is composed of positive charges throughout the surface, which reflects the lower resistivity as compared to ZIKV response [46]. ConA recognized CHIKV due to the presence of mannose residues [47]. Finally, YFV did not show significant electrochemical response due to the smallest amount of mannose or glucose in the viral structure compared to other flaviviruses [48].

YFV genome is capable of coding a polyprotein, which is post- and co-translationally processed into three structural proteins and seven non-structural proteins. The envelope (E) protein is an essential YFV structural protein and a significant component of the virion surface [49]. A previous study revealed that ConA and other lectins did not react with virus E protein, confirming the absence of sugar residues at side chains [48].

Table 1 shows the equivalent circuit parameters for the biosensor preparation and its subsequent interaction with different arboviruses (DENV2, ZIKV, CHIKV, or YFV). Our results revealed different responses for each arbovirus. Of note, our system was not responsive when negative serum was tested. This behavior demonstrated that the new biosensor is capable of recognizing virus in contaminated samples. The highest Rct values were obtained for ZIKV recognition due to the lectin specificity.

The performance of the sensor for virus detection was evaluated through the relative variation of Rct (ΔRct%). ΔRct% is an analytical component used to measure a relative impedance of the system before and after the detection process, as follows: $\Delta Rct\% = (R_{ct\ (sensor)} - R_{ct\ (virus)})/R_{ct\ (sensor)}$, where Rct_{sensor} and Rct_{virus} correspond to the sensor layer before and after arbovirus interaction, respectively [43]. PRNT was used to validate the ZIKV concentrations. Cys-ZnONp-ConA system and PRNT displayed similar responses to virus detection.

Rct is a component of the Randles circuit (inset of Fig. 3b) used to evaluate the impedance of the modified electrode. Rs and Z_W are associated with the evaluation of the electrolytic properties and the diffusion of the redox pair, respectively. Q and Rct vary with the dielectric capacity of the electrode during the electrode surface modification phases, where Q is the constant phase element, and Rct is the charge transfer resistance [33].

The interactions between a virus and lectin can be evaluated by the degree of coating of the surface (θ), represented by $\theta = 1\text{-}(R_{ct\ (sensor)}/R_{ct(virus)})$. In Fig. 5a, we observed an increase in Rct with increasing the virus' concentration. Also, a high degree of coating ($\theta \cong 80\%$) for ZIKV was obtained (Fig. 5b). Our results indicate a higher affinity of the sensor for ZIKV. The equation of limit of detection (LOD) can be expressed as LOD = 3 σ/m, where 's' is the standard deviation of the response and 'm' is the slope of a calibration curve. The LOD was calculated to be 0.0421 pfu mL^{-1} for ZIKV, 0.0437 pfu mL^{-1} for YFV, 0.062 pfu mL^{-1} for CHIKV, and 0.0382 pfu mL^{-1} for DENV.

The proposed biosensor was able to detect arboviruses in serological samples from infected patients (Fig. 6). The impedimetric response of

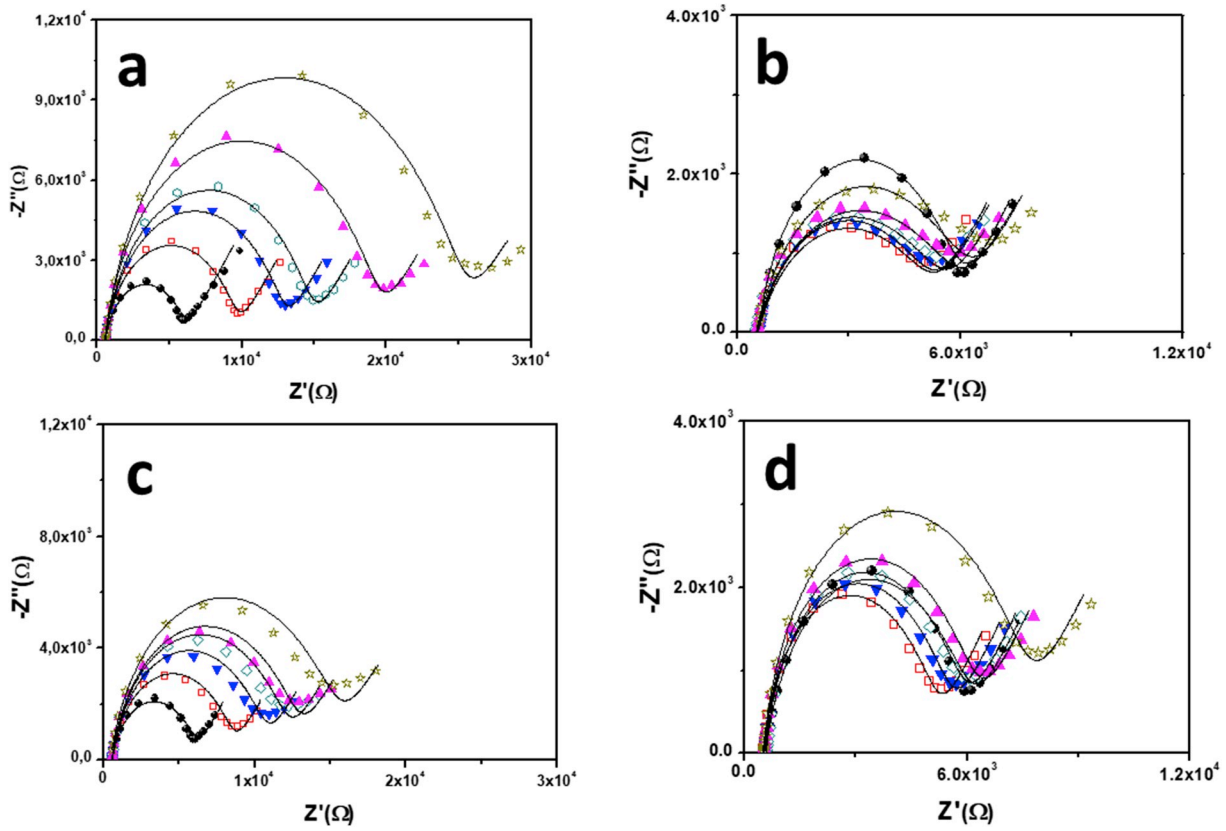

Fig. 4. Nyquist diagram of the sensor system (•) and serial dilutions of arboviruses 1:50 (□); 1:40 (∇): 1:30 (⋄); 1:20 (Δ); 1:10 (*) of the virus. ZIKV (a), DENV2 (b), CHIKV (c) and YFV (d).

Table 1
Values of the equivalent circuit elements from fitted impedance results. The analyses were performed at 1:10 dilution.

Electrode Modification	Rct (kΩ)	Rs (Ω)	Q	W	n
Au	0.35 ± 0.15	565 ± 0.28	3.73 ± 0.53	481 ± 0.22	0.79 ± 0.14
Au-Cys	4.79 ± 0.11	494 ± 0.26	1.69 ± 0.21	464 ± 0.38	0.87 ± 0.26
Au-Cys-ZnONp	0.66 ± 0.72	487 ± 0.33	2.68 ± 0.42	528 ± 0.32	0.77 ± 0.22
Au-Cys-ZnONp-ConA	2.34 ± 0.25	558 ± 0.18	1.84 ± 0.30	474 ± 0.43	0.83 ± 0.17
Au-Cys-ZnONp-ConA-BSA	5.34 ± 0.75	575 ± 0.49	1.53 ± 0.33	452 ± 0.52	0.85 ± 0.10
Sensor system-ovalbumin	14.5 ± 1.04	506 ± 0.82	8.00 ± 0.95	162 ± 0.76	0.89 ± 0.12
Sensor system-fetuin	58.7 ± 2.04	551 ± 0.94	1.38 ± 0.77	432 ± 0.31	0.86 ± 0.19
Sensor system-lactose	5.59 ± 0.70	551 ± 0.15	2.17 ± 0.32	511 ± 0.41	8.82 ± 0.17
Sensor system-glycogen	6.12 ± 0.59	511 ± 0.21	1.29 ± 0.24	433 ± 0.51	0.83 ± 0.14
ZIKV	18.6 ± 1.01	529 ± 0.71	1.26 ± 0.33	517 ± 0.44	0.87 ± 0.11
CHIKV	6.86 ± 0.23	510 ± 0.25	8.80 ± 0.93	302 ± 0.31	0.89 ± 0.23
YFV	5.98 ± 0.11	543 ± 0.23	3.75 ± 0.52	524 ± 0.12	0.74 ± 0.10
DENV2	14.6 ± 1.04	480 ± 0.37	1.15 ± 0.30	285 ± 0.51	0.86 ± 0.16
Negative serum	4.03 ± 0.23	501 ± 0.12	1.60 ± 0.22	462 ± 0.42	0.78 ± 0.20

the sensor for real samples was similar to that obtained for purified virus samples. In the case of the comparison of the ΔRct%, ZIKV exhibits the highest ΔRct% value, followed by DENV > CHIKV > YFV (Fig. 6a).

An evaluation of the n, Rct, and Q circuit elements revealed distinct viral profile to lectin recognition as observed in the 3D plot (Fig. 6b). YFV data are in the region of lower n, Rct, and Q values. Thus, YFV response is involved in a smaller blocking effect associated with smaller capacitive dispersion. CHIKV results are distributed at intermediate Rct values related to the blocking of the biosensor surface. DENV2 and ZIKV presented higher Rct values. This behavior is associated with a more significant blocking effect and smaller capacitive dispersion. The biosensor was able to differentiate arboviruses (according to saccharide structure of the viral glycoproteins) in serum from arbovirus-infected patients.

The proposed biosensor was able to identify and distinguish between arboviruses. The arboviruses produce similar proteins and therefore, can generate false-positive and false-negative results. On the other hand, the developed biosensor allows a rapid diagnosis to properly treat symptoms and identify infectious outbreaks to prevent arbovirus spreading. Our results demonstrate that ConA lectin is an active biomolecule for differentiation and identification of arboviruses due to an excellent electrochemical response for different viral glycoproteins.

4. Conclusion

In this work, a simple and sensitive electrochemical biosensor for detection and discrimination of arboviruses have been developed employing *Concanavalin A* lectin (as molecular recognition element). We demonstrated the feasibility and sensitivity of the proposed platform by

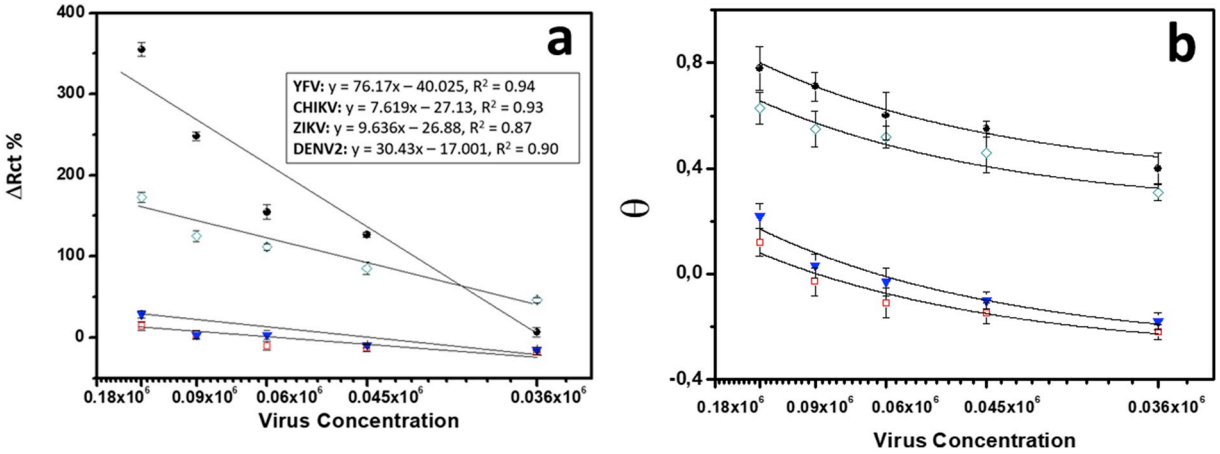

Fig. 5. ΔRct% (a) and Θ (b) as function of different dilutions of (•) ZIKV, (◇) DENV, (▽) CHIKV, and (□) YFV.

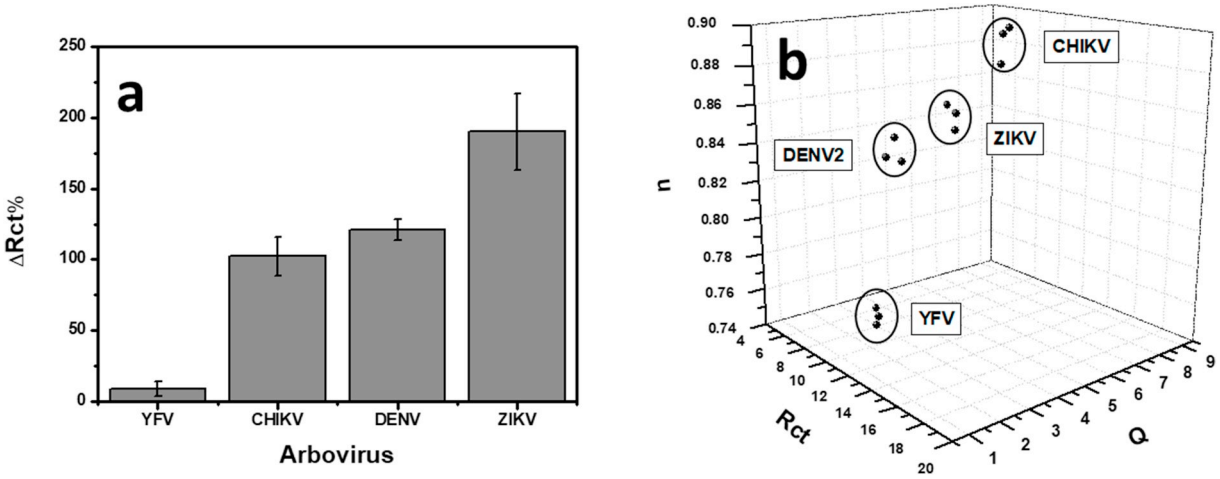

Fig. 6. ΔRct% of the biosensor exposed to samples from arboviruses-infected patients (a) and three-dimensional plot (b) for values of Rct, Q, and n given in Table 1.

using ovalbumin and fetuin as model analytes. The biosensor showed excellent analytical performance for tested arboviruses with sensitivity and wide linear range. The ConA identification of arboviruses was through interactions between carbohydrates side chains present in viral glycoproteins. The biosensor was responsive to detect arboviruses in serological samples from infected patients, even in the presence of interfering molecules. The developed biosensor was capable of differential diagnosis of arboviruses.

Acknowledgments

E.P. Simão would like to thank Foundation for Science and Technology of the State of Pernambuco (FACEPE) for a Ph.D. scholarship. L.H.V. Gil would like to thank FACEPE (grant APQ-0739-2.12/17). M.D.L. Oliveira and C.A.S. Andrade would like to thank CNPq (grant 314894/2018-7 and 314756/2018-3).

Appendix A. Supplementary data

Supplementary data to this article can be found online at https://doi.org/10.1016/j.talanta.2019.120338.

References

[1] S. Ioos, H. Mallet, I.L. Goffart, V. Gauthier, T. Cardoso, M. Herida, Current Zika virus epidemiology and recent epidemics, Medicine et Maladies Infectieuses, Med. Maladies Infect. 44 (2014) 302–307.
[2] A. Wilder-Smith, M. Quam Murray, Epidemiology of dengue: past, present and future prospects, J. Clin. Epidemiol. 5 (2013) 299.
[3] F. Deeba, A. Islam, S.N. Kazim, I.H. Naqvi, S. Broor, A. Ahmed, S. Parveen, Chikungunya virus : recent advances in epidemiology, host pathogen interaction and vaccine strategies, Pathog Dis 74 (2016) 1–10.
[4] M.R. Donalisio, I.A. Ricardo, R. Freitas, A. Paula, B. Von Zuben, Arboviruses emerging in Brazil: challenges for clinic and implications for public health, Rev. Saude Publica 51 (2017) 1–6.
[5] W. Akahata, G. Nabel, A Specific domain of the Chikungunya Virus E2 Protein regulates particle formation in human cells: implications for alphavirus vaccine design, J. Virol. 86 (2012) 8879–8883.
[6] D.F. Coe, I.F.T. Viana, M.T. Cordeiro, N. Fischer, F.F. Loe, T. Jaenisch, Mapping putative B - Cell Zika Virus NS1 epitopes provides molecular basis for anti-NS1 antibody discrimination between Zika and Dengue viruses, ACS Omega 2 (2017) 3913–3920.
[7] D. Sirohi, Z. Chen, L. Sun, T. Klose, T.C. Pierson, M.G. Rossmann, R.J. Kuhn, The 3.8 Å resolution cryo-EM structure of Zika virus, Science 352 (2016) 467–470.
[8] J.S. Dordick, R.J. Linhardt, Interaction of Zika Virus envelope protein with glycosaminoglycans, Biochemistry 56 (2017) 1151–1162.
[9] J.D. Oram, D.C. Ellwood, G. Appleyard, J.L. Stanley, Agglutination of an arbovirus by Concanavalin A, Nat. New Biol. 233 (1971) 50–51.
[10] A. Rey, Dengue virus envelope glycoprotein structure : new insight into its interactions during viral entry, Proc. Natl. Acad. Sci. U.S.A. 100 (2003) 6899–6901.
[11] E. Moulin, K. Selby, P. Cherpillod, L. Kaiser, Simultaneous outbreaks of dengue, chikungunya and Zika virus infections : diagnosis challenge in a returning traveller with nonspecific febrile illness, New Microbes New Infect 11 (2016) 6–7.
[13] CDC (U.S. Centers for Disease Control and Prevention), Types of zika virus tests, http://www.cdc.gov/zika/laboratories/types-of-tests.%0Ahtml%0A, (2016) , Accessed date: 4 May 2018.
[14] CDC (U.S. Centers for Disease Control and Prevention), Trioplex real-time RT-PCR assay, http://www.cdc.gov/zika/laboratories/types-of-tests.%0Ahtml%0A, (2016) , Accessed date: 4 May 2018.
[15] N. Oliveira, E. Souza, D. Ferreira, D. Zanforlin, W. Bezerra, M.A. Borba, M. Arruda, K. Lopes, G. Nascimento, D. Martins, M. Cordeiro, J. Lima-filho, Biosensor for the detection of specific dengue virus, Sensors 15 (2015) 15562–15577.
[16] A.M. Nicolini, K.E. Mccracken, J. Yoon, Future developments in biosensors for field-

ready Zika virus diagnostics, J. Med. Biol. Eng. 11 (2017) 1–9.
[17] H.P.O. Nascimento, M.D.L. Oliveira, C.P. De Melo, G.J.L. Silva, M.T. Cordeiro, C.A.S. Andrade, An impedimetric biosensor for detection of dengue serotype at picomolar concentration based on gold nanoparticles-polyaniline hybrid composites, Colloids Surf., B 86 (2011) 414–419.
[18] R. Khan, A. Kaushik, P.R. Solanki, A.A. Ansari, M.K. Pandey, B.D. Malhotra, Zinc oxide nanoparticles-chitosan composite film for cholesterol biosensor, Anal. Chim. Acta 616 (2008) 207–213.
[19] P. Taylor, S.A. Kumar, S.M. Chen, Nanostructured zinc oxide particles in chemically modified electrodes for biosensor applications, Anal. Lett. 41 (2008) 37–41.
[20] V. Kumar, M. Lütfi, M. Saeed, A. Osman, N. Atar, Z. Üstünda, A novel impedimetric biosensor based on graphene oxide/gold nanoplatform for detection of DNA arrays, Sens. Actuators, B 188 (2013) 1201–1211.
[21] M.L. Yola, N. Atar, A novel voltammetric sensor based on gold nanoparticles involved in p-aminothiophenol functionalized multi-walled carbon nanotubes: application to the simultaneous determination of quercetin and rutin, Electrochim. Acta 119 (2014) 24–31.
[22] M. Lütfi, T. Eren, N. Atar, A novel and sensitive electrochemical DNA biosensor based on Fe@Au nanoparticles decorated graphene oxide, Electrochim. Acta 125 (2014) 38–47.
[23] M. Lütfi, T. Eren, N. Atar, A sensitive molecular imprinted electrochemical sensor based on gold nanoparticles decorated graphene oxide : application to selective determination of tyrosine in milk, Sens. Actuators, B 210 (2015) 149–157.
[24] M.L. Yola, N. Atar, A Novel detection approach for serotonin by graphene quantum dots/two-Dimensional (2D) hexagonal boron nitride nanosheets with molecularly imprinted polymer, Appl. Surf. Sci. 458 (2018) 648–655.
[25] N. Atar, L. Mehmet, Core-Shell nanoparticles/two-Dimensional (2D) hexagonal boron nitride nanosheets with molecularly imprinted polymer for electrochemical sensing of cypermethrin, J. Electrochem. Soc. 165 (2018) H255–H262.
[26] M.L. Yola, N. Atar, Development of cardiac troponin-I biosensor based on boron nitride quantum dots including molecularly imprinted polymer, Biosens. Bioelectron. 126 (2018) 418–424.
[27] T. Yumak, F. Kuralay, M. Muti, A. Sinag, A. Erdem, S. Abaci, Preparation and characterization of zinc oxide nanoparticles and their sensor applications for electrochemical monitoring of nucleic acid hybridization, Colloids Surf., B 86 (2011) 397–403.
[28] X. Ma, J. Li, Y. Liu, Y. Yuan, G. Xu, Construction of a Concanavalin A electrochemical sensor base on a novel sandwich capture mode, Sens. Actuators, B 248 (2017) 201–206.
[29] H. Yang, H. Zhou, H. Hao, Q. Gong, K. Nie, Detection of Escherichia coli with a label-free impedimetric biosensor based on lectin functionalized mixed self-assembled monolayer, Sens. Actuators, B 229 (2016) 297–304.
[30] L. Zhao, C. Li, H. Qi, Q. Gao, C. Zhang, Electrochemical lectin-based biosensor array for detection and discrimination of carcinoembryonic antigen using dual amplification of gold nanoparticles and horseradish peroxidase, Sens. Actuators, B 235 (2016) 575–582.
[31] M.D.L. Oliveira, M.T.S. Correia, F.B. Diniz, A novel approach to classify serum glycoproteins from patients infected by dengue using electrochemical impedance spectroscopy analysis, Synth. Met. 159 (2009) 2162–2164.
[32] M.D.L. Oliveira, M.L. Nogueira, M.T.S. Correia, L.C.B.B. Coelho, C.A.S. Andrade, Detection of dengue virus serotypes on the surface of gold electrode based on Cratylia mollis lectin affinity, Sen. Actuators B 155 (2011) 789–795.
[33] C.A.S. Andrade, M.D.L. Oliveira, C.P. De Melo, L.C.B.B. Coelho, M.T.S. Correia, M.L. Nogueira, P.R. Singh, X. Zeng, Diagnosis of dengue infection using a modified gold electrode with hybrid organic – inorganic nanocomposite and Bauhinia monandra lectin, J. Colloid Interface Sci. 362 (2011) 517–523.
[34] F. Grasset, Surface modification of zinc oxide nanoparticles by aminopropyltriethoxysilane, J. Alloy. Comp. 360 (2003) 298–311.
[35] M.T. Cordeiro, C.A.A. Brito, L.J. Pena, P.M.S. Castanha, L.H.V.G. Gil, K.G.S. Lopes, R. Dhalia, J.A. Meneses, A.C. Ishigami, L.M. Mello, L.X.E. Alencar, K.M. Guarines, L.C. Rodrigues, E.T.A. Marques, Results of a zika virus (ZIKV) immunoglobulin m-specific diagnostic assay are highly correlated with detection of neutralizing anti-ZIKV antibodies in neonates with congenital disease, Braz. J. Infect. Dis. 214 (2016) 1897–1904.
[36] K.P. Nečas D, Gwyddion: an open-source software for SPM data analysis, Cent. Eur. J. Phys. 10 (2012) 181–188.
[37] J. Bouckaert, L. Wyns, V.U. Brussel, R. Loris, V.U. Brussel, Sequential structural changes upon zinc and calcium binding to metal-free Concanavalin A, J. Biol. Chem. 27 (1996) 16144–16150.
[38] R.A. Moreira, E.M.A. Pereira, M. Rita, A.J. Tatiane, A.C.O. Monteiro-moreira, R.F.O. Franc, B.A.L. Fonseca, D.F.S. Petri, Lectins and/or xyloglucans/alginate layers as supports for immobilization of dengue virus particles, Colloids Surf., B 66 (2008) 45–52.
[39] S. Ozden, M. Huerre, J. Riviere, L.L. Coffey, P. V Afonso, V. Mouly, J. De Monredon, M. El Amrani, J. Yvin, M. Jaffar, M. Frenkiel, M. Sourisseau, O. Schwartz, Human muscle satellite cells as targets of chikungunya virus infection, PLoS One 2 (2007) 527.
[40] E.P. Simão, G.J.L.S. Barbieri, C.A.S. Andrade, M.D.L. Oliveira, Biosensor based on cysteine monolayer and monoclonal antibody for specific detection of aflatoxin b1 in rice, J. Braz. Chem. Soc. 27 (2016) 1040–1047.
[41] M.D.L. Oliveira, C.A.S. Andrade, M.T.S. Correia, L.C.B.B. Coelho, P.R. Singh, X. Zeng, Impedimetric biosensor based on self-assembled hybrid cystein-gold nanoparticles and CramoLL lectin for bacterial lipopolysaccharide recognition, J. Colloid Interface Sci. 362 (2011) 194–201.
[42] S.L. Jordana, M.D.L. Oliveira, C.P. De Melo, C.A.S. Andrade, Impedimetric sensor of bacterial toxins based on mixed (Concanavalin A)/polyaniline films, Colloids Surf., B 117 (2014) 549–554.
[43] M.D.L. Oliveira, M.T.S. Correia, F.B. Diniz, Concanavalin A and polyvinyl butyral use as a potential dengue electrochemical biosensor, Biosens. Bioelectron. 25 (2009) 728–732.
[44] T.C. Pierson, B.S. Graham, Review zika Virus : immunity and vaccine development, Cell 167 (2016) 625–631.
[45] E.K.C. Kurstack, Comparative Diagnosis of Viral Diseases: Vertebrate Animal and Related Viruses, first ed., Academic Press, New York, 1981.
[46] H. Song, J. Qi, J. Haywood, Y. Shi, G.F. Gao, Zika virus NS1 structure reveals diversity of electrostatic surfaces among flaviviruses, Nature 23 (2016) 456–458.
[47] R.M. Schwartz, R. Rustandi, S. Ha, Characterization of N-glycosylation profiles from mammalian and insect cell derived chikungunya VLP, J. Chromatogr. B 1032 (2016) 2–7.
[48] L. Grubhoffer, B. Centre, C. Budejovice, Interaction of tick-borne encephalitis virus protein E with labelled lectins, in: J. Kocourek, D.L.J. Freed (Eds.), Lectins-biology, Biochemistry, Clinical Biochemistry, vol. **7**, Sigma Chem. Co., St. Louis, 2009, pp. 313–319.
[49] D.E. Volk, F.J. May, S.H.A. Gandham, A. Anderson, J.J. Von, D.W.C. Beasley, A.D.T. Barrett, D.G. Gorenstein, Structure of yellow fever virus envelope protein domain III, Virology 394 (2010) 12–18.